# An analysis of pavement heat flux to optimize the water efficiency of a pavement-watering method

Martin Hendel, Morgane Colombert, Youssef Diab, Laurent Royon

# An analysis of pavement heat flux to optimize the water efficiency of a pavement-watering method

**Martin HENDEL[1,2,3*], Morgane COLOMBERT[2], Youssef DIAB[2,4], Laurent ROYON[3]**

[1]Paris City Hall, Water and Sanitation Department, F-75014, Paris, France
[2]Université Paris-Est, EIVP, F-75019, Paris, France
[3]Univ Paris Diderot, Sorbonne Paris Cité, Laboratory MSC, UMR 7057, CNRS, F-75013, Paris, France
[4]Université Paris-Est, LEESU-GU, UMR MA 120, F-77420, Champs-sur-Marne, France
[*](corresponding author: martin.hendel@paris.fr)

Preprint version. Uploaded on May 12th, 2014.

**Abstract:** Pavement-watering as a technique of cooling dense urban areas and reducing the urban heat island effect has been studied since the 1990's. The method is currently considered as a potential tool for and climate change adaptation against increasing heat wave intensity and frequency. However, although water consumption necessary to implement this technique is an important aspect for decision makers, optimization of possible watering methods has only rarely been conducted. We propose an analysis of pavement heat flux at a depth of 5 cm and solar irradiance measurements to attempt to optimize the watering period, cycle frequency and water consumption rate of a pavement-watering method applied in Paris over the summer of 2013. While fine-tuning of the frequency can be conducted on the basis of pavement heat flux observations, the watering rate requires a heat transfer analysis based on a relation established between pavement heat flux and solar irradiance during pavement insolation. From this, it was found that watering conducted during pavement insolation could be optimized to a frequency of every 30 minutes and water consumption could be reduced by more than 76% while reducing the cooling effect by less than 10%.

## Keywords

Evaporative cooling; pavement heat flux; pavement-watering; urban heat island; climate change adaptation; heat wave

## 1. Introduction

Watering horizontal or vertical urban surfaces as a method for cooling urban spaces has been studied in Japan since the 1990s [1]–[7] and is only a recent topic in French cities such as Paris and Lyon [8]–[10]. With reported air temperature reductions ranging from 0.4°C at 2 m [9] to 4°C at 0.9 m [3], this technique is viewed as an efficient means of reducing urban heat island (UHI) intensity. In France and especially Paris, the predicted increases in heat wave intensity and frequency due to climate change [11], combined with the high sensitivity of dense cities to such episodes [12], have focused efforts on the development of appropriate adaptation tools. In parallel to techniques such as green space development, pavement-watering is seen as one of these potential tools for heat-wave adaptation in mineral areas.

Pavement-watering implies the choice of a watering method and a corresponding urban infrastructure. For any given target-area, every watering method can be characterized by three parameters: the watering period, the watering rate and the watering frequency. The former indicates the period of each day during which pavement-watering is active, the second is the average amount of water delivered per unit area and per unit time (expressed in *mm/h*, equivalent to *l/m².h*) and the last indicates the frequency of the watering cycles. Of these parameters, the watering rate is the one that defines the method's water consumption and is

Hendel, M., Colombert, M., Diab, Y., & Royon, L. (2014). An analysis of pavement heat flux to optimize the water efficiency of a pavement-watering method. *Online Preprint*. Retrieved from http://www.eivp-paris.fr/index.php/Pr%26eacute%3Bsentation?idpage=420&idmetacontenu=1191

therefore important for decision-makers who face growing public pressure to reduce urban water use.

Several watering methods have been proposed or studied in the existing literature. In 2008, the City of Paris financed a numerical research program aimed at testing different climate change adaptation strategies for heat wave events [8]. This work analyzed a daytime pavement-watering method based on a hypothetical infrastructure connected to the city's non-potable water network. Pavements and sidewalks were watered at a rate of 0,2 *mm/h* for a duration of 3 minutes and frequency of every hour. During this work, a nighttime watering experiment was conducted over the summer of 2012 [9]. A single watering cycle of the pavement and sidewalk was conducted by cleaning truck around 10 pm sprinkling 1 *l/m²*, which is estimated by city officials as the maximum retention capacity of standard Parisian pavements. Field studies conducted in Nagoaka City, Japan used an existing snow-melting infrastructure which consists of a ground-water network used to water the road surface. Kinouchi & Kanda [1] ran this system continuously at a rate of 11 *mm/h*, while Takahashi et al. [3] ran it intermittently to deliver an average 2 *mm/h* with 3-minute sprinkles, every 30 minutes. Yamagata et al. [4] used reclaimed waste water sprinkled onto a water-retentive pavement by temporary pipes placed on a central road planter. The watering method parameters are not specified in this study or in any of the other cited studies.

Of these, only Takahashi et al. [3] and Météo-France & CSTB [8] describe attempts to optimize the watering method with atmospheric cooling parameters. Takahashi et al. [3] optimize both watering rate and frequency based on surface and 90-cm air temperature observations over a period of one hour after watering. Météo-France & CSTB [8] base their own optimization on findings from Takahashi et al. with the hypothesis of a pavement water-holding capacity of 1 *mm*. They optimize the watering rate based on 2-m air temperature simulations with a one-hour time step.

We propose to optimize an adapted version of Bouvier et al.'s [9] pavement-watering method by studying the pavement's thermal behavior. We will demonstrate how pavement heat flux measurements can be used to fine-tune the watering frequency, and how a surface heat transfer analysis combined with a linear relation found between heat flux and solar irradiance during pavement insolation can provide information on the watering rate. Measurements were obtained from one of two experimental sites in Paris over the summer of 2013. For this campaign, the rue du Louvre was equipped with a ground heat flux and temperature sensor which was placed 5 cm below the pavement surface as well as a pyranometer, and was watered several times during the day.

## 2. Materials and Methods

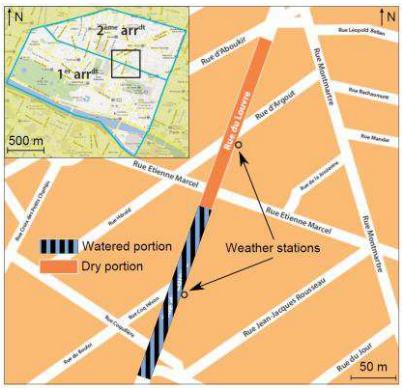


Figure 1: *Map of the rue du Louvre site*

Conductive heat flux and surface temperatures were investigated on rue du Louvre, near Les Halles in the 1st and 2nd Arrondissements in Paris, France over the summer of 2013. Watered and control weather station positions are illustrated in Figure 1. Both watered and dry portions of the street are approximately 180 m long and 20 m wide. Rue du Louvre has an aspect ratio approximately equal to 1 and has a N-NE – S-SW orientation.

All data is presented in local daylight savings time (UTC +2). Statistical analyses were conducted using the R software environment, version 3.0.1. Because the control site was vandalized and thus rendered unoperational early during the experimental period, only watered station data on watered and dry (control) days will be discussed hereafter.

## 2.1. Instruments

The pavement at each site was equipped with a thermo-fluxmeter at a depth of 5 cm. This sensor was connected to a weather station which functioned continuously for the duration of the summer and was used for additional microclimatic measurements which will not be discussed here. Figure 2 illustrates a top view of sensor installation. The weather station was positioned at the Eastern end of the cable.

The sensor was placed in the middle of the North-bound bus lane, causing no traffic disturbances once installed. Unauthorized parking and a 100-m distant traffic light ensured that only very limited shading or localized heat exhaust was caused by vehicles. Figure 3 shows a detailed cross-section of how the pavement sensor was set in place before filling.

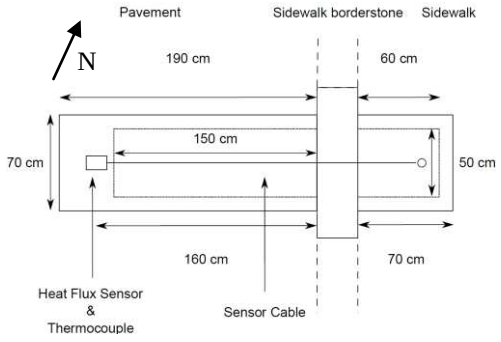


Figure 2: *Top view of pavement sensor*

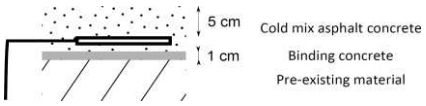


Figure 3: *Cross-section detail of pavement sensor filling materials*

Table 1 summarizes the instruments and data used for our upcoming analyses.

| Parameter | Instrument | Height | Accuracy |
|---|---|---|---|
| Solar irradiance | Second Class Pyranometer ISO 9060 | 4 m | 10% daily |
| Pavement heat flux | Taylor-made flowmeter | -5 cm | 5% |

Table 1: *Instrument type, measurement height and accuracy*

## 2.2. Watering method and optimization goals

Watering was started if certain weather conditions were met based on Météo-France's three-day forecast. These as well as those for heat-wave warnings are presented in Table 2.

Cleaning trucks were used to sprinkle approximately 1 *mm* every hour from 6:30 am to 11:30 am and every 30 minutes from 2 pm until 6:30 pm on the sidewalk and pavement. This

is considered to be the maximum water-holding capacity of the pavement. Watering times were reported by truck operators and cross-checked against visible images taken by a rooftop thermal camera. Resulting watering time precision is estimated to be no better than 5 minutes.

Water used for this experiment was supplied by the city's 1,600-km non-potable water network, principally sourced from the Ourcq Canal. Although water temperature was not measured, its summertime range is reported by city services to be 20°-25°C.

| Parameter | Pavement-watering | Heat-wave warning level |
|---|---|---|
| Mean 3-day minimum air temperature ($BMI_{Min}$) | > 16°C | > 21°C |
| Mean 3-day maximum air temperature ($BMI_{Max}$) | > 25°C | > 31°C |
| Wind speed | < 10 *km/h* | - |
| Sky conditions | Sunny (less than 2 oktas cloud cover) | - |

Table 2: *Weather conditions required for pavement-watering and heat wave warnings*

In this situation, the goals we set for our pavement-watering optimization were:

- Maximize the obtained pavement cooling effect
- Minimize water consumption
- Minimize the watering frequency to limit disturbances caused by cleaning trucks

Direct pavement heat flux analysis is sufficient for the frequency optimization, while a heat transfer analysis is necessary to estimate the effect of pavement-watering and to optimize the water consumption. The heat transfer analysis requires a preliminary analysis of pavement heat flux measurements.

## 2.3. Heat transfer analysis

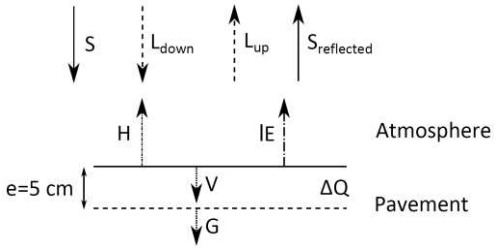


Figure 4: *Diagram of pavement heat budget at surface*

For the rest of this article, we refer to pavement heat flux density at a depth of 5 cm as *G*, solar irradiance measured by the pyranometer at a height of 4 m as *S'* and that received by the pavement as *S*. All measurements are made at 1-minute intervals. Figure 4, based on Kinouchi & Kanda [2], shows a diagram of the heat fluxes relevant to this experiment. Heat absorption by the water film is not illustrated but is taken into account in the last item of equation (3).

Asaeda et al. [13] and Kinouchi & Kanda [2] characterize the energy balance of the pavement surface by the following equations:

$$R_n = S + L_{down} - L_{up} - S_{reflected} \quad (1)$$

$$R_n^{dry} = H^{dry} + V^{dry} \ (dry) \quad (2)$$

$$R_n^{wet} = H^{wet} + V^{wet} + lE + c\rho\frac{V_s}{t_0}(T_S^{wet} - T_W)\ (wet) \quad (3)$$

$$V = G + \Delta Q \quad (4)$$

$R_n$ is the net downward radiation received by the pavement surface and is the sum of the downward solar irradiance $S$, downward longwave radiation $L_{down}$ and upward longwave radiation $L_{up}$ and reflected shortwave radiation $S_{reflected}$; $H$ is the upward sensible heat flux; $V$ is the downward pavement heat flux at the surface; $l$ is the latent heat of vaporization for water (2,260 *J/g*); $E$ is the evaporation rate; $c$ is the specific heat of water (4.18 *kJ/kg.K*); $\rho$ is the density of water (1,000 $kg/m^3$); $V_S$ is the water volume dispersed per unit surface area (1 $l/m^2$); $t_0$ is the water cycle period in seconds; $T_W$ is the water temperature; $\Delta Q$ is the heat storage flux by the first 5-cm layer of pavement.

According to Jurges' formula [14], convective heat flux can be written as:

$$H = h(T_S - T_{air}) \quad (5)$$

Where $T_S$ is the surface temperature of the pavement and $T_{air}$ is that of the air above it. $h$ is the convective heat transfer coefficient.

Several empirical formulae exist to calculate $h$ based on wind speed, $v$ (in *m/s*). These include $h$=6.15+4.18$v$ used by Kusaka et al. [15] and $h$=5.7+3.8$v$ in Duffie & Beckman [16]. Under our conditions, $h$ is approximately equal to 10 *W/m.K*.

From these equations, the following can be derived when comparing dry and wet surface conditions under equal insolation:

$$lE + c\rho\frac{V_s}{t_0}(T_S^{wet} - T_W) = h\left(T_S^{dry} - T_S^{wet} + T_{air}^{wet} - T_{air}^{dry}\right) + V_{dry} - V_{wet} + L_{up}^{dry} - L_{up}^{wet} \quad (6)$$

From Stefan-Boltzmann law, we can express $L_{up}$ as:

$$L_{up} = \varepsilon\sigma T_S^4 \quad (7)$$

$\varepsilon$ is the emissivity of the emitting surface, while $\sigma$ is Boltzmann's constant.

Therefore, knowledge of $G$, $\Delta Q$, air, water and pavement surface temperatures under dry and wet conditions allows an estimation of the latent heat flux and thus the evaporation rate.

## 2.4. Derivation of pavement solar irradiance from 4-meter solar irradiance

*S'* was measured continuously starting on July 2nd, 2013. Because of the difference in positioning of the pyranometer and the pavement sensor, *S'* is not equal to *S* and can therefore not be used in its place for the heat transfer analysis. We must therefore derive *S* from *S'*.

Apart from possible insolation interruptions due to road traffic not visible in *S'*, the only difference is the insolation period. The visible images taken by an infrared rooftop camera reveal a 20-minute-long time lag between the beginning of pavement sensor and pyranometer insolation during the month of July. The time lag is immediately identifiable when comparing the graphs of *G* and *S'* for July 11th in Figure 5 and Figure 6. The beginning and end of pavement and pyranometer insolation are illustrated by the two dotted and dashed vertical lines in Figure 6, respectively. These coincide with the sudden increases and declines seen in each signal. The insolation period of the pavement is approximately 1:35 pm to 6:30 pm, while that of the pyranometer is 1:55 pm to 6:50 pm. We suppose that no signal distortion other than the time lag is at play.

With these hypotheses, a modification of *S'* during the two 20-minute exclusive disjunctions of pyranometer and pavement insolation is undertaken to obtain *S*. The rest of the

signal is unchanged, apart for distortions due to vehicles. Finally, to ensure signal continuity, the 5 minutes following and/or preceding these 20-minute periods are also modified.

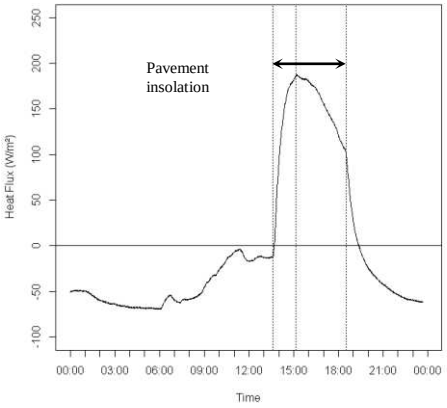


Figure 5: G *measured on July 11th*

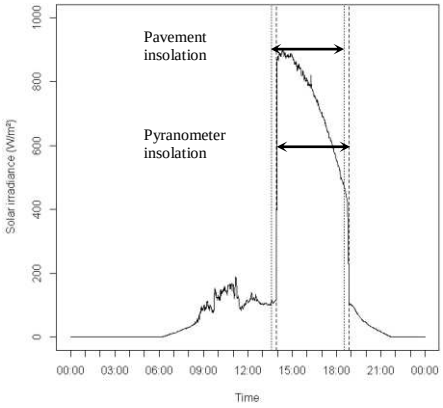


Figure 6: S' *measured on July 11th*

# 3. Watering period and frequency

Pavement heat flux density data from the watered station will now be compared between watered days and days without watering (control days). These observations will help infer conclusions on the watering frequency. All selected days are of Pasquill Stability Class A (i.e. strong daytime insolation and surface wind speeds below 2 *m/s*) [17].

## 3.1. Results

### *3.1.1. Control days*

The evolution of *G* and *S* on July 11th, 14th, and 20th are presented in Figure 7 through Figure 12. *S* ranges from 0 *W/m²* to 120 *W/m²* during shading and from 120 *W/m²* to 900 *W/m²* during direct insolation. *G* ranges from -60 *W/m²* to 200 *W/m²*.

In terms of heat flux, each day can be divided into three periods: two of net heat release ($G<0$) in the morning and evening and one of net heat storage ($G>0$) during the day. The net release of heat by the pavement lasts about 18 hours, while heat is during the remaining 6 hours, approximately between 1:30 pm and 7 pm.

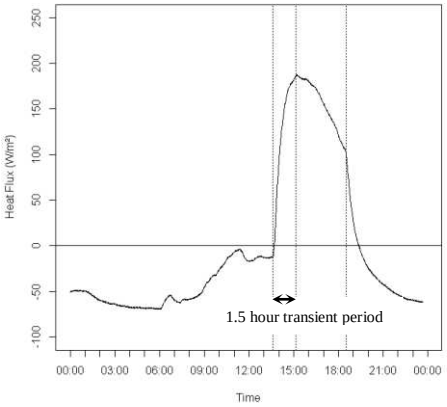


Figure 7: G *measured on July 11th*

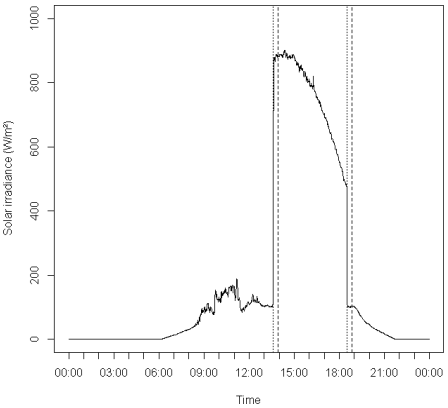


Figure 8: S *measured on July 11th*

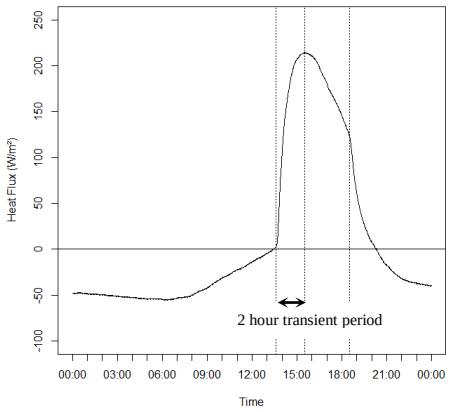


Figure 9: G *measured on July 14th*

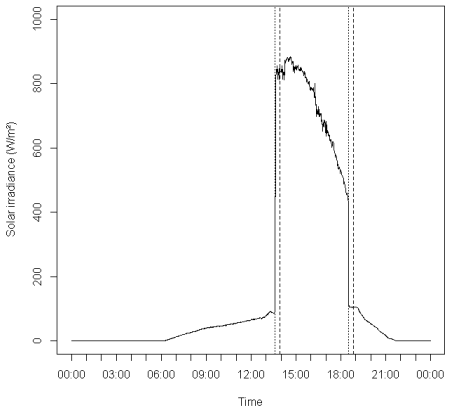


Figure 10: S *measured on July 14th*

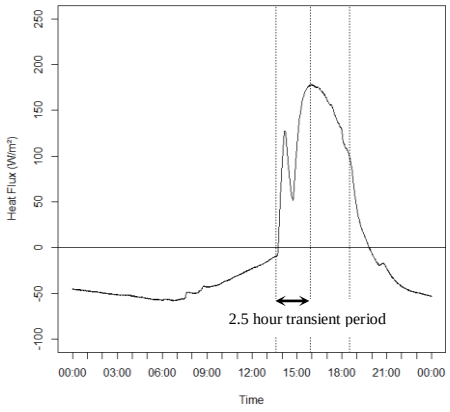


Figure 11: G *measured on July 20th*

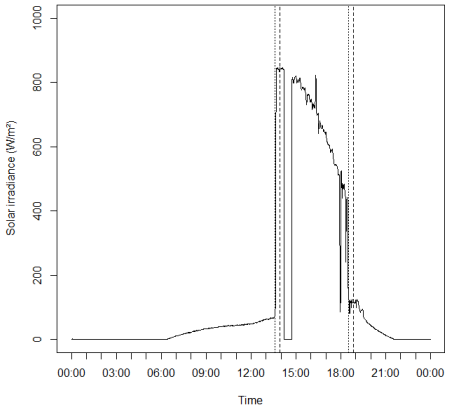


Figure 12: S *measured on July 20th*

When the sun starts to hit the pavement, *G* enters a transient period during which the top 5 cm layer of pavement begins to store heat, i.e. during which $\Delta Q \neq 0$. The transient period is outlined by the first two dotted vertical lines in Figures 12, 14 and 16. The last dotted vertical line indicates the instant when the pavement is shaded, at approximately 6:30 pm. After the transient period, *G* and *S* follow a similar trend.

### *3.1.2. Watered days – July 8th, 10th and 22nd*

Watered days will now be considered in the following order: July 8th, 22nd and 10th. Figure 13 through Figure 18 illustrate *G* and *S* on those dates, respectively. Dot-dashed vertical lines represent watering cycles. *S* is in the same range as found on control days, while *G* ranges from -75 *W/m²* to 130 *W/m²*.

The maximum value of *G* is about half that reached on control days, ranging from 70 *W/m²* to 130 *W/m²*, approximately half that observed on control days. The daily peak in *G* is found to coincinde with the beginning of afternoon watering, except on July 10th when afternoon watering began simultaneously to insolation. Furthermore, the observed reduction is inversely proportional to the delay between the start of afternoon watering and the start of pavement insolation. In other words, the later afternoon pavement-watering begins, the higher the daily peak in *G*.

The watering methods applied in the afternoon on those dates and the daily maximum value of *G* is summarized in Table 3. Watering cycles occurred at the specified frequencies except for a 50-minute interruption on July 22nd at approximately 3 pm.

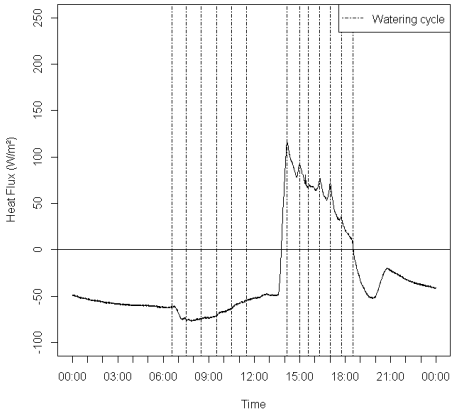


Figure 13: G *measured on July 8th*

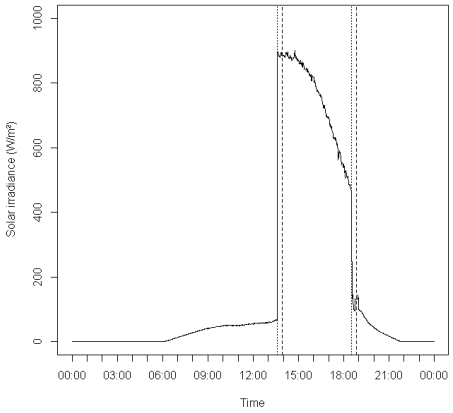


Figure 14: S *measured on July 8th*

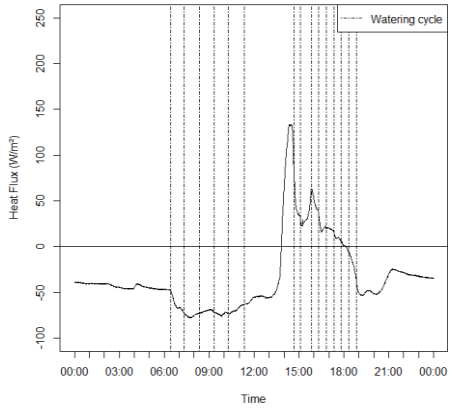


Figure 15: G *measured on July 22nd*

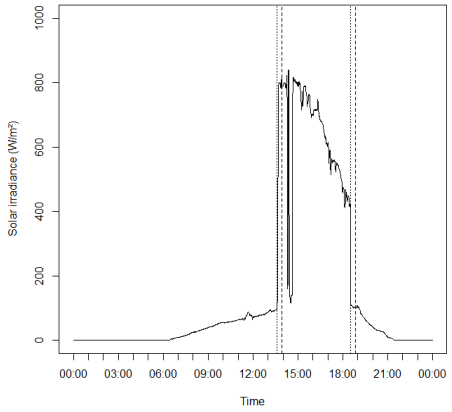


Figure 16: S *measured on July 22nd*

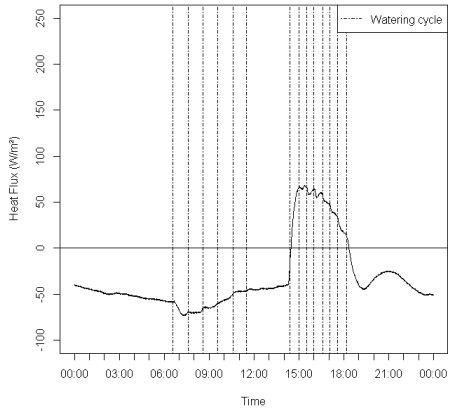


Figure 17: G *measured on July 10th*

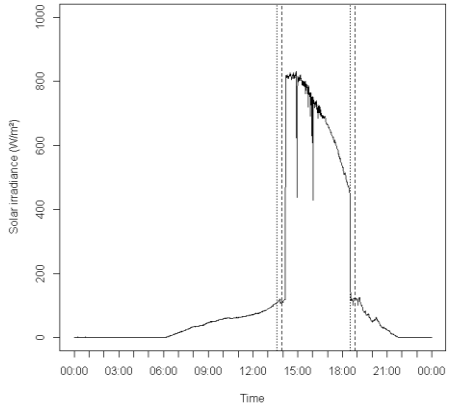


Figure 18: S *measured on July 10th*

215

| Watering method parameter | July 8th | July 22nd | July 10th |
|---|---|---|---|
| Watering rate (*mm/h*) | 1.33 | 2 | 2 |
| Watering period (*minutes*) | 45 | 30 | 30 |
| Delay of watering vs. start of insolation (*minutes*) | 35 | 65 | <5 |
| Daily maximum value of *G* (*W/m²*) | 115 | 130 | 70 |

216 Table 3: *Actual watering method on considered watered days*

Between 3 pm and 6:30 pm, the average reduction in pavement heat flux compared to different reference control days is found to be between 100 and 150 *W/m²*. Table 4 summarizes these reductions. In the morning, *G* is reduced by approximately 15 *W/m²*.

| Date | July 8th | | July 22nd | | July 10th | |
|---|---|---|---|---|---|---|
| Control day (reference) | July 11th | July 14th | July 14th | July 20th | July 11th | July 14th |
| Average reduction (*W/m²*) | -100 | -120 | -130 | -150 | -110 | -130 |

Table 4: *Average heat flux density reduction in* W/m² *on watered days*

Additionnally, small heat flux spikes are observed in the afternoon on July 8th and 22nd. Those that occur after the beginning of afternoon pavement-watering coincide with watering cycles occuring 45 minutes or longer after the previous cycle. On July 10th, when watering is conducted every 30 minutes without interruption, these spikes are significantly smaller than on July 8th and 22nd. In the morning, no significant heat flux spikes are visible on watered days, except for minor ones on July 10th.

Compared to control days, pavement-watering shortens the net heat storage period ($G>0$) by between 1 and 1.5 hours. This is caused by an earlier end of the net storage period, while the beginning of heat storage is unaffected. On July 10th, pavement insolation was delayed by a parked vehicle. Furthermore, pavement heat flux dips sharply at 6:30 pm when shading begins and increases again 1-2 hours later, when the pavement surface dries.

### 3.2. Discussion

The comparison of *G* on watered days with control days revealed strong effects due to pavement-watering. On the one hand, heat flux density reductions were found to be highest in the afternoon during pavement insolation with *G* being more than halved. The average reduction is between 100 and 150 *W/m²* during this period. Morning heat flux density, when the pavement is shaded, was also reduced by pavement-watering in the order of 15 *W/m²*. On the other hand, the daily peak in *G* was found to coincide with the first afternoon watering cycle and to be proportional to the delay between this cycle and pavement insolation. Furthermore, spikes in *G* were observed if watering cycles were more than 45 minutes apart.

This provides insight on two aspects of the watering method: its watering period and its frequency. First, the value of the daily maximum of *G* depends on the start of afternoon watering relatively to pavement insolation. Second, if the pavement watering frequency is too low, the pavement surface has enough time to dry and *G* rises towards its normal control value until the next watering cycle.

In order to maximize pavement cooling in the afternoon, watering should begin just a few minutes prior to pavement insolation. Furthermore, the watering frequency must be adjusted to prevent the pavement surface from drying. Our observations suggest that a period of 45 minutes is too long, while 30 minutes is nearly optimal during insolation. In the morning, in shaded conditions, our data suggests that watering every hour is sufficient, perhaps optimal.

Overall, our observations are consistent with preivous work. On control days, the trend in heat flux is comparable to measurements made without pavement-watering by Kinouchi & Kanda [2], also 5 cm deep, although inside a porous pavement. Our measurements are about twice as large as what Asaeda et al. [13] observed 20 cm below the asphalt pavement surface. Given the difference in depth, this discrepancy is not considered surprising. On watered days, our observations are similar to those of Kinouchi & Kanda [1], [2] as well: the first watering

cycle on all watered days coincides with a small "nose-dive" in *G* in the order of 15 *W/m²*. Lastly, the net storage period is shorter in our experiment than in reports from Kinouchi & Kanda [2] or Asaeda et al. [13], but they were working in nearly unmasked conditions.

# 4. Watering rate

Kinouchi & Kanda [2] put into perspective a correlation between $R_n$ and *G*. They proceeded by plotting *G* as a function of $R_n$. Camuffo & Bernardi [18] explore the hysteris cycles found between surface heat fluxes and net radiation for soil. Other authors such as Asaeda et al. [13], studying the effect of pavement heat storage on the lower atmosphere, also look into this hysteris cycle for asphalt and concrete pavements. Because we did not measure net radiation, we shall procede in an analoguous fashion with *S* instead. This will allow us to estimate the surface cooling effect of pavement watering based on a relation between *S* and *G* during pavement insolation. From this we get an estimate of the evaporation rate and therefrom we can make recommendations on the watering rate.

## 4.1. Results

Figure 19 through Figure 24 show *G* as a function of *S* on July 11th, 14th, 20th, 8th, 22nd and 10th, respectively. The chronological order of the data points is anti-clockwise. The least square regression line of *G* according to *S* between 3 pm and 6:30 pm is plotted for each date.

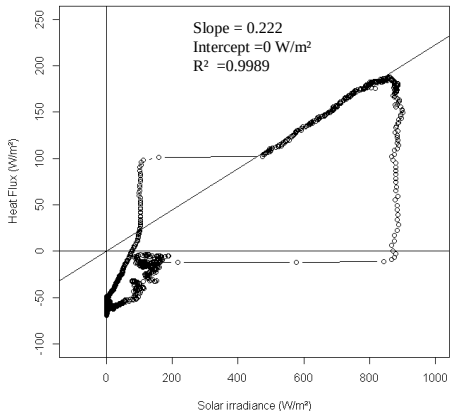


Figure 19: G *as a function of* S *on July 11th*

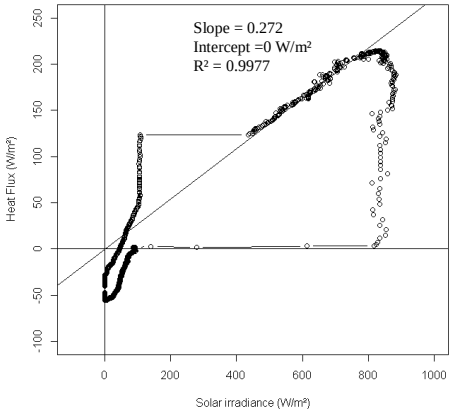


Figure 20: G *as a function of* S *on July 14th*

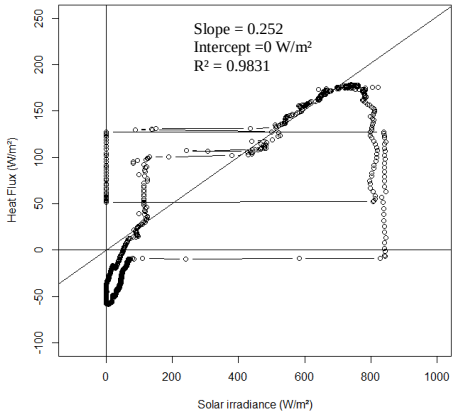


Figure 21: G *as a function of* S *on July 20th*

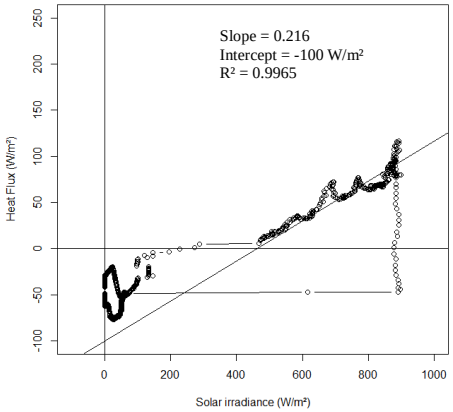


Figure 22: G *as a function of* S *on July 8th*

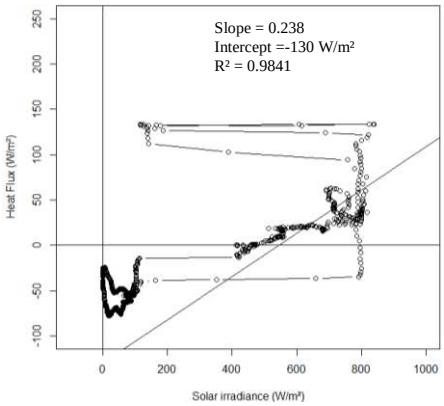


Figure 23: G *as a function of* S *on July 22nd*

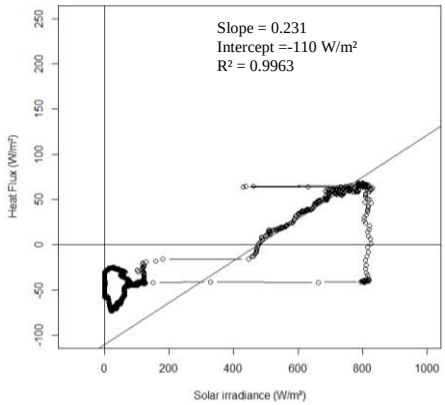


Figure 24: G *as a function of* S *on July 10th*

The parameters from the linear regression can be formalized as:

$$G = \alpha S + G_0 \quad (8)$$

$\alpha$ is the conversion coefficient of solar irradiance to pavement heat flux 5 cm below the pavement surface, while $G_0$ is the intercept heat flux under these conditions.

The regressions were conducted for control and watered days. On control days, an intercept of 0 *W/m²* was used. Table 5 summarizes the regression parameters for control days.

| Date | July 11th | July 14th | July 20th |
|---|---|---|---|
| $\alpha$ | 0.222 | 0.272 | 0.252 |
| $R^2$ | 0.9989 | 0.9977 | 0.9831 |

Table 5: α *and* R² *on control days*

Each fit is statistically significant, with coefficients of determination in excess of 0.98. Overall, the conversion coefficients derived on control days range from 22% to 27%.

On watered days, different intercepts, corresponding to the average reduction of *G* found in Table 4, were tested. Using these intercepts, similar slopes to those found on control days were obtained. Table 6 summarizes the regression parameters using the different intercepts for watered days.

Regardless of the intercept value used, the conversion coefficients deviate only slightly from those derived on control days, remaining in the same 22-27% range.

| Date | July 8th | | July 22nd | | July 10th | |
|---|---|---|---|---|---|---|
| Control day | July 11th | July 14th | July 14th | July 20th | July 11th | July 14th |
| $G_0$ (*W/m²*, user-input) | -100 | -120 | -130 | -150 | -110 | -130 |
| $\alpha$ | 0.216 | 0.244 | 0.238 | 0.269 | 0.231 | 0.261 |
| $R^2$ | 0.9965 | 0.9955 | 0.9861 | 0.9849 | 0.9959 | 0.9953 |

Table 6: α, R² *and* $G_0$ *on watered days*

Considering the statistical significance of these regression parameters, we conclude that pavement-watering does not significantly affect the conversion coefficient, i.e. how solar energy is transmitted 5 cm deep into the pavement, but adds a constant negative heat flux, $G_0$.

Based on observations by Kinouchi & Kanda [2] and this unmodified conversion rate, we shall assume that $\Delta Q$ is also unchanged by watering during insolation, i.e. $\Delta Q^{wet} = \Delta Q^{dry}$.

This information allows us to estimate the cooling created by the sprinkled water. We find that the contribution from water advection is between 23 and 35 *W/m²*, while that of evaporation is 304-375 *W/m²*. This is produced by the evaporation of 0.48 to 0.60 *mm/h*. Advection is therefore responsible for less than 10% of observed cooling while it is provided by up to three times more water than evaporative cooling.

This is derived by using the regression parameters to express *G* as a linear function of *S* during steady state insolation conditions:

$$G = \alpha S + G_0 \delta_{wet} \quad (9)$$

In equation (9), $\delta_{wet}$ is the wet pavement indicator function. In dry surface conditions, $\delta_{wet} = 0$, while in wet surface conditions $\delta_{wet} = 1$.

Integrating equations (7) and (9) into (6), we obtain:

$$lE + c\rho\frac{V_s}{t_0}(T_S^{wet} - T_W) = h\left(T_S^{dry} - T_S^{wet} + T_{air}^{wet} - T_{air}^{dry}\right) - G_0 + \sigma\left(\varepsilon_d {T_S^{dry}}^4 - \varepsilon_w {T_S^{wet}}^4\right) \quad (10)$$

As stated in the introduction, previous studies of pavement-watering report air temperature reductions of up to 4°C [1]–[4], [9]. For our analysis, we assume that $-2°C \leq T_{air}^{wet} - T_{air}^{dry} \leq 0$

In addition, collected pavement surface temperature data (not discussed here) reveal an average reduction during insolation of 15°C, from 323 *K* to 308 *K*. Having assumed that *h* = 10 *W/m².K*, and considering that $110\ W/m^2 \leq -G_0 \leq 150\ W/m^2$ on days with the optimal 30-minute watering, we obtain:

$$339\ W/m^2 \leq lE + c\rho\frac{V_s}{t_0}(T_S^{wet} - T_W) \leq 399\ W/m^2$$

As stated previously, we know from past non-potable water analyses conducted by the city services that its temperature is usually in the 20-25°C range on hot summer days. Assuming that the runoff temperature increases to 35°C by contact with the pavement, we obtain:

$$\begin{cases} 23\ W/m^2 \leq c\rho\frac{V_s}{t_0}(T_S^{wet} - T_W) \leq 35\ W/m^2 \\ 304\ W/m^2 \leq lE \leq 375\ W/m^2 \end{cases}$$

Considering a latent heat of evaporation of 2,260 *kJ/kg*, we can assert that the evaporation rate is between 0.134 and 0.166 *g/m².s*, i.e. between 0.48 and 0.60 *mm/h*. This means that for each 30-minute watering cycle, 0.24 to 0.30 *mm* evaporate. Since we know from our preliminary pavement heat flux analysis that the pavement dries off after 30 minutes, we can assert that the rest of the water runs off into the sewer system.

### 4.2. Discussion

The analysis of *G* as a function of *S* during insolation after the initial transient period has allowed us to demonstrate that pavement-watering accounts for 339 to 399 *W/m²* of pavement surface cooling. At least 90% of total cooling attributable to pavement-watering is produced by evaporation, up to 10% being produced by water advection.

The relative contributions of advection and evaporation contrast strongly with the amount of water used by each of these phenomena which is respectively 2 *mm/h* and 0.48 to 0.60 *mm/h*. Pavement cooling by water advection is therefore much less water efficient than that from evaporation: 12 to 18 *W/m²* of cooling per 1 *mm/h* of sprinkled water, compared to 628 *W/m²* per 1 *mm/h* of evaporated water.

Since evaporative cooling cannot be increased by adding more water, increasing the watering rate further would only increase the advective contribution. However, in light of its low cooling efficiency, this is unadvisable for our optimization goal. On the contrary, we would recommend lowering the watering rate to match the evaporation rate exactly. This would lower advective cooling to between 6 and 10 *W/m²*, bringing total pavement-watering cooling down to between 309 and 386 *W/m²*, i.e. a 3-9% reduction for a 70-76% water saving.

Our estimations of latent heat flux are consistent with those reported by Météo-France & CSTB [8] who find that latent heat flux can reach 300 *W/m²*. Furthermore, they found an optimal watering rate of 0.2 *mm/h* for all of Paris' road surfaces. This value was obtained by testing different watering rates with a frequency of every hour and a water-holding capacity of 1 *mm*. However, it is a daily and city average for watering every hour between 5 am and 7 pm and is not more accurately defined for individual street configurations. Furthermore, the authors were limited in the choice of the watering frequency since the model's time step was one hour and was found sufficient considering a water-holding capacity of 1 *mm*. Our findings are therefore consistent with theirs.

Another consequence of our results is information on the water-holding capacity of the pavement. Since the pavement dries 30 minutes after watering during insolation, the water-holding capacity of the pavement is therefore equal to the amount of water evaporated in between 30-minute watering cycles, i.e. between 0.24 and 0.30 *mm*. This is significantly less than that assumed by Météo-France & CSTB [8], but is only valid for the portion of pavement surveyed by the heat flux sensor. This portion has a specific geometric configuration and surface composition (cold- versus hot-mix asphalt concrete). However, we can still assert that the optimized watering method applies the exact water-holding capacity of the target pavement-area at the frequency that it takes for that amount of water to completely evaporate. Thus, if we assume that the watering frequency used in the morning is optimal, we can estimate morning evaporation to 0.24 to 0.30 *mm/h*.

Sources of uncertainty in our estimations lie in the use of $S$ rather than $R_n$, the approximation of the convective heat transfer coefficient $h$ and our assumptions regarding water temperature, air temperature changes and the storage heat flux density in dry and wet conditions. Concerning the latter, observations over several days by Kinouchi & Kanda [2] suggest that $\Delta Q$ is unaffected by pavement watering under identical insolation conditions.

## 5. Conclusion

The field study conducted on rue du Louvre in Paris over the summer of 2013 has allowed us to expose the thermal effects of pavement-watering on a pavement area located 1.6 m away from the eastern sidewalk in a street with an aspect ratio of H/W=1 and of N-NE – S-SW orientation. Pavement heat flux density at 5 cm depth was found to be more than halved by pavement-watering during insolation, while a heat transfer analysis based on a linear relation found between solar irradiance and heat flux density allowed us to estimate evaporative cooling to between 304 and 375 *W/m²*, representing at least 90% of total pavement-watering cooling. This translates to an evaporation rate of between 0.48 and 0.60 *mm/h*. Assuming that the one-hour morning watering cycles were optimal, the evaporation rate during morning

shaded conditions is 0.24 to 0.30 *mm/h*. Finally, we found that the water-holding capacity of the surveyed pavement zone is 0.24 to 0.30 *mm*.

Based on these analyses, we recommend watering the exact water-holding capacity of the pavement at the lowest possible frequency that prevents the pavement from drying. In our case, this translates to 30-minute watering cycles with a watering rate of 0.48 to 0.60 *mm/h* during pavement insolation. In the morning, 60-minute watering cycles and a watering rate of 0.24 to 0.30 *mm/h* are recommended. Compared to our experiment, this watering method would use 76% less water while still providing at least 90% of observed pavement cooling. Finally, the watering period should include a few minutes right before pavement insolation to maximize the cooling effect.

In order to reduce the watering frequency further and thus cause less disturbance associated with watering cycles, the pavement water-holding capacity would need to be increased. As Parisian streets are currently designed to evacuate surface water as fast as possible, a change in street design is necessary to meet this objective. One alternative that can be considered is to use water-retaining pavement materials. The new street material would have to store water at or near its surface without preventing evaporation. Such a material would permit the delivery of larger amounts of water per watering cycle with lower runoff and thus reduce the watering frequency. In addition, the new road structure may be able to store rainfall from summer storms or water already used for street cleaning long enough for evaporation on hot days. This would lead to additional water savings all while having positive impacts on rainwater runoff management.

Water temperature, net radiation and sensible heat flux measurements as well as the determination of the thermal characteristics of the pavement material would help address the sources of uncertainty in our analysis. In addition, these measurements would allow us to verify our conjecture on optimal watering during pavement shading via a similar approach to that used for the afternoon.

## References


[1] T. Kinouchi and M. Kanda, "An Observation on the Climatic Effect of Watering on Paved Roads," *J. Hydrosci. Hydraul. Eng.*, vol. 15, no. 1, pp. 55–64, 1997.

[2] T. Kinouchi and M. Kanda, "Cooling Effect of Watering on Paved Road and Retention in Porous Pavement," in *2nd Symposium on Urban Environment*, 1998, pp. 255–258.

[3] R. Takahashi, A. Asakura, K. Koike, S. Himeno, and S. Fujita, "Using Snow Melting Pipes to Verify the Water Sprinkling's Effect over a Wide Area," in *NOVATECH 2010*, 2010, p. 10.

[4] H. Yamagata, M. Nasu, M. Yoshizawa, A. Miyamoto, and M. Minamiyama, "Heat island mitigation using water retentive pavement sprinkled with reclaimed wastewater.," *Water Sci. Technol.*, vol. 57, no. 5, pp. 763–71, Jan. 2008.

[5] T. Nakayama and T. Fujita, "Cooling effect of water-holding pavements made of new materials on water and heat budgets in urban areas," *Landsc. Urban Plan.*, vol. 96, no. 2, pp. 57–67, May 2010.

[6] T. Nakayama, S. Hashimoto, and H. Hamano, "Multiscaled analysis of hydrothermal dynamics in Japanese megalopolis by using integrated approach," *Hydrol. Process.*, vol. 26, no. 16, pp. 2431–2444, Jul. 2012.

[7] J. He and A. Hoyano, "A numerical simulation method for analyzing the thermal improvement effect of super-hydrophilic photocatalyst-coated building surfaces with water film on the urban/built environment," *Energy Build.*, vol. 40, no. 6, pp. 968–978, Jan. 2008.

[8] Météo-France and CSTB, "EPICEA - Rapport final," 2012.

[9] M. Bouvier, A. Brunner, and F. Aimé, "Nighttime watering streets and induced effects on the surrounding refreshment in case of hot weather. The city of Paris experimentations," *Tech. Sci. Méthodes*, no. 12, pp. 43–55 (In French), 2013.



Hendel, M., Colombert, M., Diab, Y., & Royon, L. (2014). An analysis of pavement heat flux to optimize the water efficiency of a pavement-watering method. *Online Preprint*. Retrieved from http://www.eivp-paris.fr/index.php/Pr%26eacute%3Bsentation?idpage=420&idmetacontenu=1191

[10] J. Nicolas, “Reducing the urban heat island effect,” *Le Moniteur*, 2013. [Online]. Available: http://www.lemoniteur.fr/133-amenagement/article/actualite/22580961-experimentation-reduire-l-effet-d-ilot-de-chaleur-urbain. [Accessed: 22-Jan-2014].
[11] A. Lemonsu, R. Kounkou-Arnaud, J. Desplat, J.-L. Salagnac, and V. Masson, “Evolution of the Parisian urban climate under a global changing climate,” *Clim. Change*, vol. 116, no. 3–4, pp. 679–692, Jul. 2012.
[12] J.-M. Robine, S. L. K. Cheung, S. Le Roy, H. Van Oyen, C. Griffiths, J.-P. Michel, and F. R. Herrmann, “Death toll exceeded 70,000 in Europe during the summer of 2003.,” *C. R. Biol.*, vol. 331, no. 2, pp. 171–8, Feb. 2008.
[13] T. Asaeda, V. T. Ca, and A. Wake, “Heat storage of pavement and its effect on the lower atmosphere,” *Atmos. Environ.*, vol. 30, no. 3, pp. 413–427, Feb. 1996.
[14] W. Jürges, “Die Wärmeübergang an einer ebenen Wand,” *Beihefte zum Gesundheits-Ingenieur*, vol. 19, no. 1, pp. 1227–1249, 1924.
[15] H. Kusaka, H. Kondo, and Y. Kikegawa, “A simple single-layer urban canopy model for atmospheric models : comparison with multi-layer and slab models,” *Boundary-Layer Meteorol.*, vol. 101, no. 3, pp. 329–358, 2001.
[16] J. A. Duffie and W. A. Beckman, *Solar Engineering of Thermal Processes*, 2nd Editio. New York, 1991, p. 944.
[17] F. Pasquill, “The estimation of the dispersion of windborne material,” *Meteorol. Mag.*, vol. 90, no. 1063, pp. 33–49, 1961.
[18] D. Camuffo and A. Bernardi, “An observational study of heat fluxes and their relationships with net radiation,” *Boundary-Layer Meteorol.*, vol. 23, no. 3, pp. 359–368, Jul. 1982.

## Acknowledgements

The authors would like to thank APUR for lending their Flir TiR32 infrared camera and Orange for allowing the use of their rooftop terrace located at 46, rue du Louvre for instruments used during this experiment. They also acknowledge the support of Météo-France and APUR as well as the Green Spaces and Environment, Roads and Traffic and the Waste and Water Divisions of the City of Paris during the preparation phase of this experiment.

Funding for this experiment was provided for by the Water and Sanitation Department of the City of Paris.

## Nomenclature

| | |
|---|---|
| $\alpha$ | conversion coefficient of solar irradiance to pavement heat flux density at 5 cm depth, - |
| *APUR* | Parisian urban planning agency |
| $BMI_{Min}$ | Minimum biometeorological index, 3-day mean of daily low temperature, *°C* |
| $BMI_{Max}$ | Maximum biometeorological index, 3-day mean of daily high temperature, *°C* |
| $c$ | water specific heat, 4.18 *J/g.K* |
| $\Delta Q$ | storage heat flux density by top 5-cm layer of pavement, *W/m²* |
| $e$ | pavement thickness above the heat flux sensor, *5 cm* |
| $E$ | evaporation rate, *g/s* |
| $\varepsilon_d$ | dry pavement emissivity, 0.97 |
| $\varepsilon_w$ | wet pavement emissivity, 0.98 |
| $G$ | downward conductive heat flux density, 5 cm below the pavement surface, *W/m²* |
| $H$ | upward sensible heat flux density at pavement surface, *W/m²* |
| $h$ | convection coefficient, *W/m².K* |
| $\ell$ | latent evaporation heat of water, 2,260 *kJ/kg* |
| $L_{down}$ | downward longwave radiation density, *W/m²* |
| $L_{up}$ | upward longwave radiation density, *W/m²* |
| *MRT* | mean radiant temperature, *°C* |
| $R_n$ | net radiation density, *W/m²* |
| $\rho$ | water density, 1,000 *kg/m³* |

| | | |
|---|---|---|
| 478 | $S$ | pavement solar irradiance, $W/m^2$ |
| 479 | $S'$ | pyranometer solar irradiance, $W/m^2$ |
| 480 | $S_{reflected}$ | reflected shortwave radiation density, $W/m^2$ |
| 481 | $T_{air}$ | atmospheric air temperature, $°C$ |
| 482 | $T_S$ | pavement surface temperature, $°C$ |
| 483 | $T_w$ | water temperature, $°C$ |
| 484 | $t_0$ | watering cycle period, *hours* |
| 485 | $V$ | pavement conductive heat flux density, at surface, $W/m^2$ |
| 486 | *UHI* | urban heat island |